Work and dissipation fluctuations near the stochastic resonance of a colloidal particle

Pierre Jop, Sergio Ciliberto, Artyom Petrosyan

Work and dissipation fluctuations near the stochastic resonance of a colloidal particle

Pierre Jop, Artyom Petrosyan & Sergio Ciliberto

Université de Lyon, Laboratoire de Physique de l'École Normale Supérieure de Lyon, CNRS UMR 5276, , 46 allée d'Italie, 69364 Lyon cedex 7, France.

PACS 05.40.-a – Fluctuation phenomena, random processes, noise, and Brownian motion
PACS 05.70.Ln – Nonequilibrium and irreversible thermodynamics
PACS 82.70.Dd – Colloids

Abstract. - We study experimentally the fluctuations of the injected and dissipated energy in a system of a colloidal particle trapped in a double well potential periodically modulated by an external perturbation. The work done by the external force and the dissipated energy are measured close to the stochastic resonance where the injected power is maximum. We show that the steady state fluctuation theorem holds in this system.

A colloidal particle, confined in a double well potential, hops between the two wells at a rate r_k, named the Kramers' rate, which is determined by the height δU of the energy barrier between the two wells, specifically $r_k = \tau_o^{-1} \exp(-\frac{\delta U}{k_B T})$, where τ_o is a characteristic time, k_B the Boltzmann constant and T the heat bath temperature [1]. When the double well potential U is modulated by an external periodic perturbation whose frequency is close to r_k the system presents the stochastic resonance phenomenon [2], i.e. the hops of the particle between the two wells synchronize with the external forcing. The stochastic resonance has been widely studied in many different systems and it has been shown to be a bona fide resonance looking at the resident time [2, 3] and the Fourier transform of the signal for different noise intensity [4]. Numerically, the stochastic resonance has been characterized by computing the injected work done by the external agent as a function of noise and frequency [5, 6]. However the fluctuations of the injected and dissipated power at the stochastic resonance have never been studied experimentally. This is a very important and general issue within the context of Fluctuation Theorems (FT) which constitute extremely useful relations for characterizing the probabilities of observing entropy production or consumption in out of equilibrium systems. These relations were first observed in the simulations of a sheared fluid [7] and later proven both for chaotic dynamical systems [8] and for stochastic dynamics [9]. These works lead to different formulations which find powerful applications for measuring free-energy difference in biology (see e.g. [10] for a review). The hypothesis and the extensions of fluctuation theorems [11] have been tested in various experimental systems such as colloidal particles [12–14], mechanical oscillators [15], electric circuits [16] and optically driven single two-level systems [17]. The effect of nonharmonic potential on the motion of a colloidal particle has been tested by Blickle *et al.* [13, 17, 18]. However the kind of nonharmonic potential used in these experiments did not induce a bistable dynamics of the Brownian particle, and as far as we know there is only one experimental study of FT for bistable systems which are not thermally activated [17]. Recently a numerical study, which has explored the distributions of the dissipated heat and of the work in a Langevin dynamics near the stochastic resonance, has shown that FT holds in the long-time limit [19, 20].

To give more insight into this problem we study experimentally the Steady State Fluctuation Theorem (SSFT) in the case of a colloidal bistable system, composed by a Brownian particle trapped in a double well potential periodically modulated by an external driving force. We measure the energy injected into the system by the sinusoidal perturbation and we analyze the distributions of work and heat fluctuations. We find that although the dynamics of the system is strongly non-linear the SSFT holds for the work integrated on time intervals which are only a few periods of the driving force.

The experimental setup is composed by a custom built vertical optical tweezers made of an oil-immersion objec-

tive (63×, N.A.=1.3) which focuses a laser beam (wavelength $\lambda = 1064$ nm) to the diffraction limit for trapping glass beads (2 μm in diameter). The silica beads are dispersed in bidistilled water in very small concentration. The suspension is introduced in the sample chamber of dimensions $0.25 \times 10 \times 10\ mm^3$, then a single bead is trapped and moved away from others. The position of the bead is tracked using a fast-camera with the resolution of 108 nm/pixels which gives after treatment the position of the bead with an accuracy better than 20 nm. The trajectories of the bead are sampled at 50 Hz.

The position of the trap can be easily displaced on the focal plane of the objective by deflecting the laser beam using an acousto-optic deflector (AOD). To construct the double well potential the laser is focused alternatively at two different positions at a rate of $5kHz$. The residence times τ_i (with $i = 1, 2$) of the laser in each of the two positions determine the mean trapping strength felt by the trapped particle. Indeed if $\tau_1 = \tau_2 = 100\mu s$ the typical diffusion length of the bead during this period is only 5 nm. As a consequence the bead feels an average double-well potential: $U_0(x) = ax^4 - bx^2 - dx$, where a, b and d are determined by the laser intensity and by the distance of the two focal points. In our experiment the distance between the two spots is 1.45 μm, which produces a trap whose minima are at $x_{min} = \pm 0.45\mu m$. The total intensity of the laser is 58 mW on the focal plane which corresponds to an inter-well barrier energy $\delta U_o = 1.8\ k_BT$. Starting from the static symmetric double-trap, ($\tau_1 = \tau_2$) we modulate the depth of the wells at low frequency by modulating the residence times (τ_i) during which the spot remains in each position[1]. The modulation of the average intensity is harmonic at frequency f and its amplitude $(\tau_2 - \tau_1)/(\tau_2 + \tau_1)$, is 0.7 % of the average intensity in the static symmetric case. Thus the potential felt by the bead has the following profile in the axial direction:

$$U(x,t) = U_0(x) + U_p(x,t) = U_0 + c\ x\ \sin(2\pi f t), \qquad (1)$$

with $ax_{min}^4 = 1.8\ k_BT$, $bx_{min}^2 = 3.6\ k_BT$, $d|x_{min}| = 0.44\ k_BT$ and $c|x_{min}| = 0.81\ k_BT$. The amplitude of the time dependent perturbation is synchronously acquired with the bead trajectory.[2]

An example of the measured potential for $t = \frac{1}{4f}$ and $\frac{3}{4f}$ is shown on the Fig. 1a). This figures is obtained by measuring the probability distribution function $P(x,t)$ of x for fixed values of $c\sin(2\pi f t)$, it follows that $U(x,t) = -\ln(P(x,t))$.

The x position of the particle can be described by a Langevin equation:

$$\gamma\dot{x} = \frac{dU}{dx} + \xi, \qquad (2)$$

[1]We keep the total intensity of the laser constant in order to produce a more stable potential.

[2]The parameters given here are average parameters since the coefficients a, b and c ,obtained from fitted steady distributions at given phases, vary with the phase ($\delta a/a \approx 10\%$, $\delta b/b \approx \delta c/c \approx 5\%$).

with $\gamma = 1.61\ 10^{-8} N\ s\ m^{-1}$ the friction coefficient and ξ the stochastic force. The natural Kramers' rate ($c = 0$) for the particle is $r_k = 0.3Hz$ at $T = 300K$. When $c \neq 0$ the particle can experience a stochastic resonance when the forcing frequency is close to the Kramers' rate. An example of the sinusoidal force with the corresponding position are shown on the figure 1b). Since the synchronization is

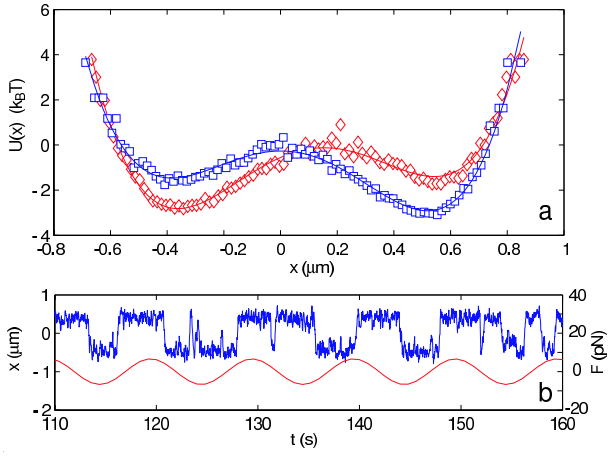

Fig. 1: a) The perturbed potential at $t = \frac{1}{4f}$ and half a forcing period later. b) Example of trajectory of the glass bead and the corresponding perturbation at $f = 0.1$ Hz.

not perfect, sometimes the particle receives energy from the perturbation, sometimes the bead moves against the perturbation leading to a negative work on the system.

In the following, all energies are normalized by k_BT. From the trajectories, we compute the stochastic W_s and the classical W_{cl} works done by the perturbation on the system and the heat Q exchanged with the bath. These three quantities are defined by the following equations as in ref. [21]:

$$\begin{aligned} W_s[x(t)] &= \int_{t_0}^{t_0+t_f} dt \frac{\partial U(x,t)}{\partial t} \\ W_{cl}[x(t)] &= -\int_{t_0}^{t_o+t_f} dt \dot{x} \frac{\partial U_p(x,t)}{\partial x} \\ Q[x(t)] &= -\int_{t_0}^{t_0+t_f} dx \frac{\partial U(x,t)}{\partial x} \end{aligned} \qquad (3)$$

where in this case $t_f = \frac{n}{f}$ is a multiple of the forcing period. We use both W_s and W_{cl} because they give complementary informations on the fluctuations of the energy injected by the external perturbation into the system (see ref. [22] and reference therein for a discussion on this point). For example, as we will see later, W_s/T is the total entropy production rate in this specific case [23]. The heat and the work, defined in eq.3, are related through the first principle of thermodynamics: $Q = -\Delta U + W_s$, where $\Delta U = U(x(t_f + t_0), t_0 + t_f) - U(x(t_0), t_0)$, whereas the two works are related by a boundary term $W = -\Delta U_p + W_s$, where $\Delta U_p = U_p(x(t_f + t_0), t_f + t_0) - U_p(x(t_0), t_0)$. We

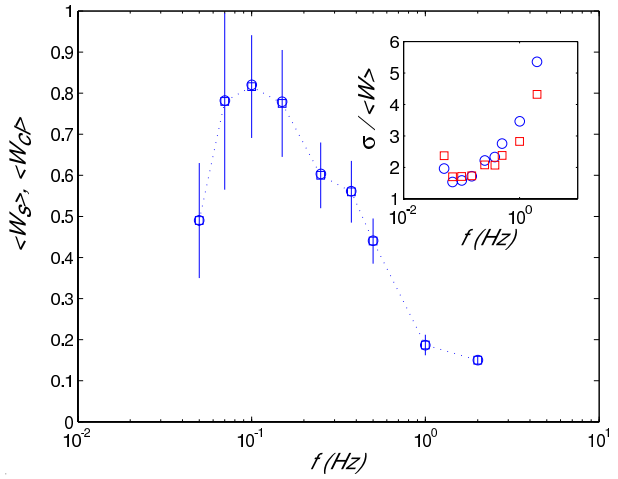

Fig. 2: Injected energy in the system over a single period as a function of the driving frequency (W_s □ and W_{cl} ○). The error bars are computed from the standard deviation of the mean over different runs. Inset: Standard deviations of work distributions over a single period normalized by the average work as a function of the frequency (same symbols).

first measure the average work received over one period for different frequencies ($t_f = \frac{1}{f}$ in eq. 3). Each trajectory is here recorded during 3200 s in different consecutive runs, which corresponds to 160 up to 6400 forcing periods, for the range of frequencies explored. In order to increase the statistics we consider 10^5 different t_o. The figure 2 shows the evolution of the mean work per period for both definitions of the work. First, the input average work decreases to zero when the frequency tends to zero. Indeed, the bead hops randomly several times between the two wells during the period. Second, in the limit of high frequencies, the particle has not the time to jump on the other side of the trap but rather stays in the same well during the period, thus the input energy is again decreasing when increasing frequency. In the intermediate regime, the particle can almost synchronize with the periodical force and follows the evolution of the potential. The maximum of injected work is found around the frequency $f \approx 0.1$ Hz, which is comparable with half of the Kramers' rate of the fixed potential $r_K = 0.3$ Hz. This maximum of transferred energy shows that the stochastic resonance for a Brownian particle is a bona fide resonance, as it was previously shown in experiments using resident time distributions [3, 24] or directly in simulations [5, 6]. It is worth noting that the average values of work in this case do not depend on their definitions: only the boundary terms, which vanish in average with time, are different. In the inset of figure 2, we plot the normalized standard deviation of work distributions ($\sigma / \langle W \rangle$) as a function of the forcing frequency. The curves present a minimum at the same frequency of 0.1 Hz, in agreement again with the resonance phenomena. However, we observe a difference between the two quantities. This underlines that these measured works have not identical fluctuations, which will be studied in detail in the following of the article. We now focus on the distributions of work over a single period. On the figures 3, we present the probability density function (PDF) of W_s and W_{cl} for different frequencies. One can notice the presence of a single bump around the mean value for low frequency (Fig. 3a), in agreement with the behavior of the bead. The fluctuations reach values, which are larger than six times the average injected work. Due to the lack of events during an experiment at such low frequency, we are not allowed to conclude about the shape of the distribution. However, it seems to tend to a gaussian distribution with deviations for large fluctuations. Close to the resonance frequency (Fig. 3b), the distribution is wide and shifted toward a larger value. Then, when the frequency increases (Fig. 3c), the distribution shows several peaks. For the classical work, the first peak, centered around zero, corresponds to the work received when the bead does not leave its well during the period. The other one corresponds to the work done on the system during a single jump of the bead. For higher frequencies (Fig. 3d), only the central peak remains and increases, the distributions become more symmetrical and tends to a gaussian centered on zero since the bead hardly leaves its well and thus explores only the energy landscape of one well. Although the mean works are equal, the distribution of W_s and W_{cl} present significant differences close to the stochastic resonance. In order to study in more details these distributions of work and heat dissipation, we choose a frequency of external driving (0.25 Hz) which ensures a good statistic, by allowing the observation of the system over a sufficient number of periods, and which, at the same time, produces a non trivial distribution (see Fig. 3). We compute the works and the

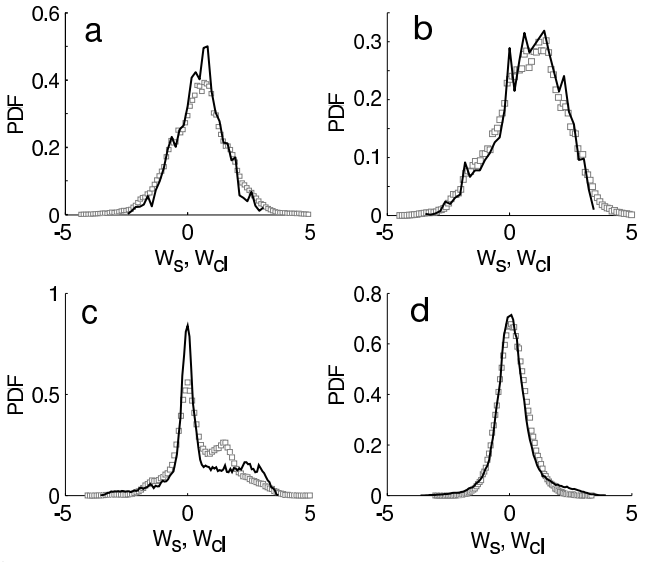

Fig. 3: Distributions of work over one period of W_{cl} (symbols) and W_s (solid line) for a forcing at a) 0.05 Hz, b) 0.1 Hz, c) 0.375 Hz and d) 2 Hz.

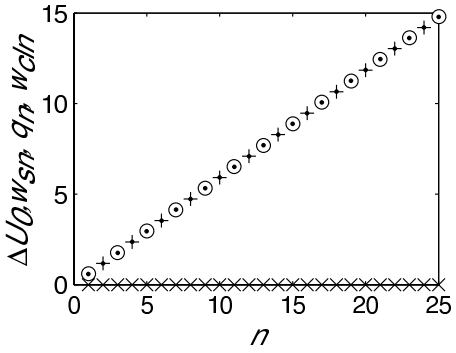

Fig. 4: Evolution of the mean value of works($\circ$, $\bullet$), dissipation ($+$) and potential variations ($\times$) over an increasing number of period n ($f = 0.25$ Hz).

dissipation using 1.5 10^6 different t_o on time series which spans about 7500 period of the driving. The quantities W_{sn}, W_{cln} and Q_n refer to averages made over n periods of the driving. The exchanged heat is defined from the first principle of the dynamic: $\Delta U_0 = W_{cl} - Q$. The figure 4 shows first the linear increase of W_{sn}, W_{cln} and Q_n with n and second that all these quantities are equals because ΔU_0 vanishes in average (shown by the crosses in Fig. 4). The distribution of ΔU_0 is plotted in Fig. 5. We

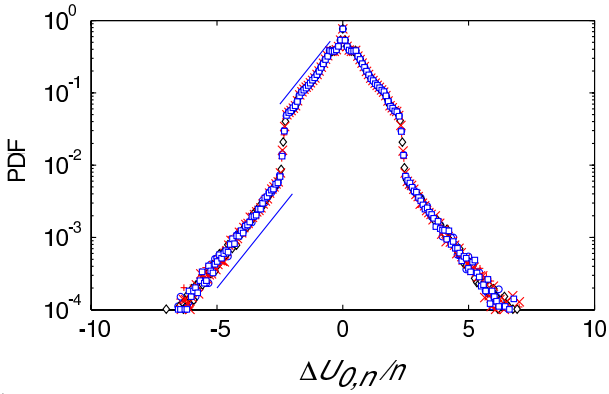

Fig. 5: Distribution of ΔU_0 for $n = 1, 2, 4, 8, 12$. The lines are proportional to $\exp(-\Delta U_0)$ ($f = 0.25$ Hz).

observe first that these distributions do not depend on the number of integration period. This is due to the fact that the potential depends only on the position at the end of the n-th period, which has the same distribution for all n. We notice the classical large exponential wings preceded by a sudden decrease in the distribution. This breakdown corresponds to the potential energy of the inter-well barrier and could be understood as follow: The bead can not explore so often the high values of the potential as in a single well configuration but jumps likely into the other well. We can also remark secondary peaks around zero, which correspond to a small difference of energy between the two wells. Each peak correspond to the probability of having a single jump during driving period. For small values of ΔU_0, the PFD decreases also exponentially, describing the evolution of the bead in a single trap. We

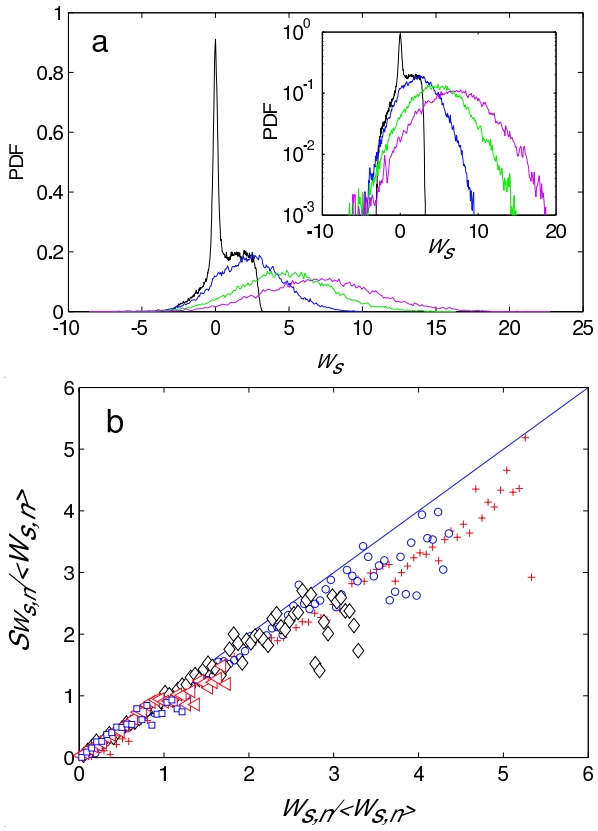

Fig. 6: a) Distribution of stochastic work for different number of period $n = 1$, 4, 8 and 12 ($f = 0.25$ Hz). Inset: Same data in lin-log. b) Normalized symmetry function as function of the normalized work for $n = 1$ ($+$), 2 ($\circ$), 4 ($\diamond$), 8 ($\triangle$), 12 ($\square$).

discuss in the following the PDFs $P(X_n)$ of X_n where X_n stands for one of the three variables W_{sn}, W_{cln} and Q_n. For these quantities we also study the SSFT which states that:

$$S_{X_n} = \log(\frac{P(X_n = w)}{P(X_n = -w)}) \rightarrow w \text{ for } n \rightarrow \infty \qquad (4)$$

where S_{X_n} is called the symmetry function. It is important to notice that Eq. 4 for W_{sn} should hold for all n. Indeed taking into account that $Q_n = -\Delta U + W_{sn}$ it is easy to realize that in this case W_{sn}/T is just the total entropy production defined by Seifert [18,23] who has shown that that for this quantity the SSFT holds for any integration time which is an integer number of periods of the forcing.

We consider first $P(W_{sn})$ which is plotted in Fig 6a) for various n. The distribution presents a sharp peak for $n = 1$, which disappears as soon as n increases. The distribution then tends to a gaussian for high values of n. To directly test the SSFT, we plot $S_{W_{sn}}/ < W_{sn} >$ as a funtion of $W_{sn}/ < W_{sn} >$ in Fig. 6b). It is remarkable that

straight lines are obtained even for n close to 1, where the distribution presents a very complex and unusual shape. These curves seem to collapse on the curve $y = x$. We

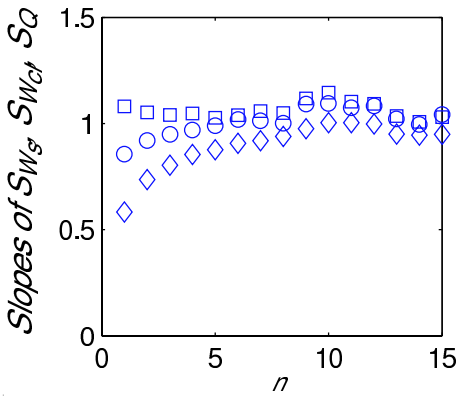

Fig. 7: Slope at the origin of the symmetry functions of W_{sn} ($\circ$) ,W_{cln} ($\square$) and Q_n ($\diamond$) as function of n ($f = 0.25$ Hz).

have looked closer to the slope of $S_{W_{sn}}$ for small work fluctuations. Its evolution is shown on the figure 7. The SSFT is not verified at small n but it is rapidly valid for increasing number of periods. The convergency turns out to be much faster than that observed in a harmonic oscillator [15] where SSFT is satisfied only for $n > 30$. This is indeed an important point because as we have already mentioned W_{sn}/T corresponds, in this case, to the total entropy production, for which SSFT has to be verified for all n [23]. Thus the statistical and numerical uncertainties could explain the fact that in our data and in those of ref. [19] the slope of $S_{W_{sn}}$ versus W_{sn} for $n = 1$ is not exactly one. Indeed in ref. [25] it has been shown that even in the gaussian case it is required a very large statistical accuracy in the calculation of the total entropy to satisfy SSFT for small n. In our case this accuracy has to be larger than in the gaussian case because of the extremely complex shape of the $P(W_{sn})$ for n=1. For the classical definition of the work W_{cln}, the fluctuations are larger than those of W_{sn} (Fig. 8a). Again, the distributions tend to a gaussian for large n (inset of Fig. 8a). On Fig. 8b), we have plotted the normalized symmetry function of W_{cln}. We can see that the curves are close to the line of slope one. For high values of work, the dispersion of the data increases due to the lack of events. The slopes at the origin are shown in Fig. 7. We can see an increase of the slope near zero and then an oscillation. Although we can not average over more periods, the slope seems to tends toward 1 as expected by the SSFT. The strong analogy existing between the convergency of W_{sn} and W_{cl} is probably due to the fact that, as already mentioned, they differ only for a boundary term that rapidly goes to zero when n is increased. Now, we consider the heat fluctuations. The PDFs show even larger fluctuations (Fig 9). We can notice first that the PDFs decrease exponentially in the asymptotic limit. This is due to the exponential

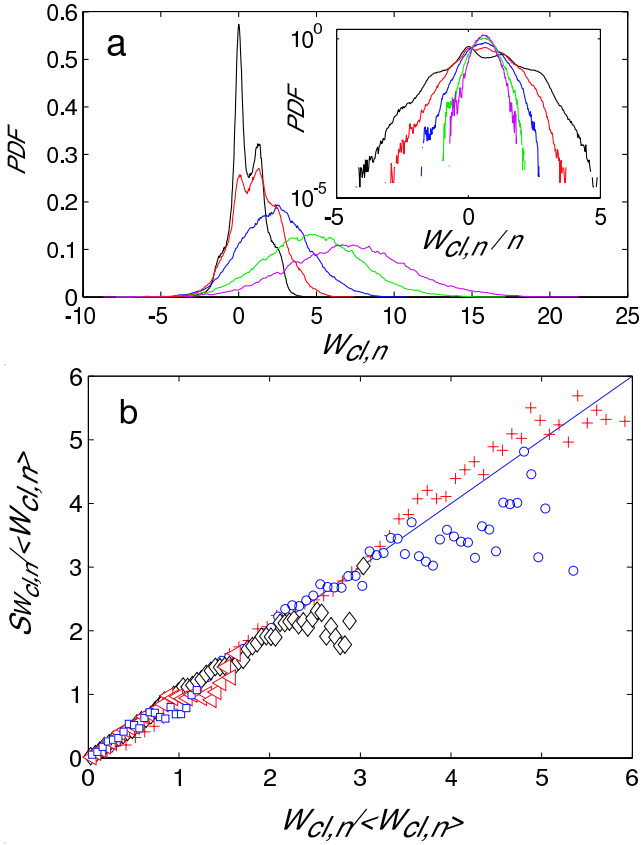

Fig. 8: a) Distribution of classical work W_{cl} for different numbers of period $n = 1$, 2, 4, 8 and 12 ($f = 0.25$ Hz). Inset: Same data in lin-log. b) Symmetry function as function of the normalized work (same symbols as in Fig. 6.)

tails of the distribution of ΔU_0 that become predominant. This behavior is less pronounced for higher values of n. Near the maximum, these distributions tend to be gaussian as shown by the exponential fit (dashed line). On the figure 9b), the symmetry function of the dissipated heat is shown as function of the dissipated heat. We can define two regions, in the first one, the curve increases linearly and then bents. On the inset of Fig. 9b), which shows the normalized symmetry function of Q_n, the two different regimes appear clearly. First, the slope of the linear part increases with n and goes asymptotically toward 1, as shown on Fig. 7. Only the linear part for $Q_n < 3$ has been fitted. Starting near 0.6 for one period, it grows toward 1 more slowly than for the classical work. This shows that the SSFT holds asymptotically when n increases for $Q_n \ll \langle Q_n \rangle$. On the other regime, one could expect the curve to reach the value 2 from the shape of the exponential tails. However, their size are too small to create a horizontal asymptote. Still, when normalizing the data by the average of Q_n (inset of Fig. 9b), the data begin to explore the second regime around a value compatible with the value 2, that would need longer measurements (over more period) to be confirmed.

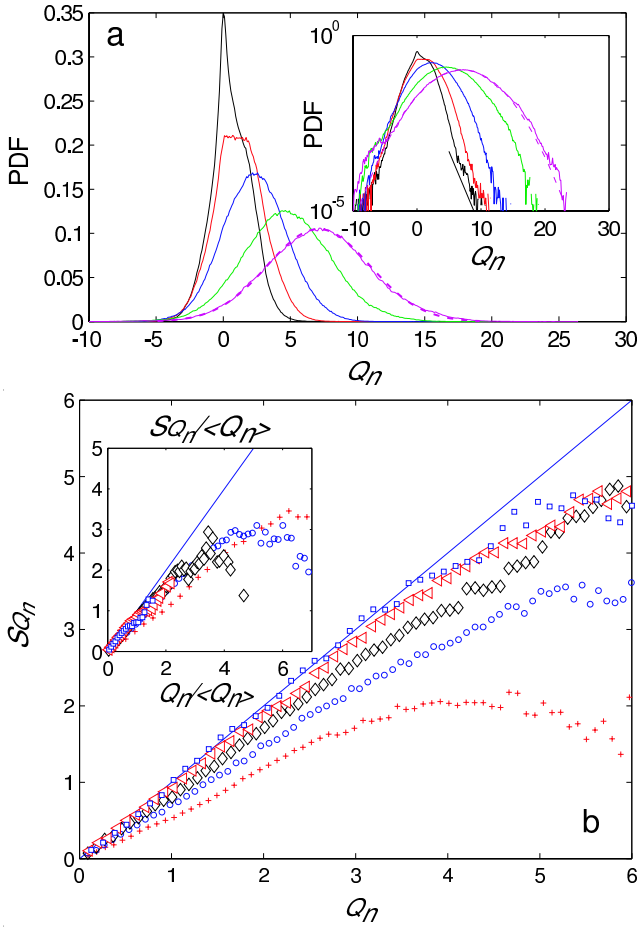

Fig. 9: a) Distribution of the dissipation for different numbers of period $n = 1$, 2, 4, 8 and 12. The straight line is proportional to $exp(-Q_n)$. The dashed line is a gaussian fit of the PDF for $n = 12$. Inset: Same data in lin-log . b) Symmetry function of the dissipation for $n = 1$, 2, 4, 8 and 12. Inset: normalized symmetry function ($f = 0.25$ Hz). (same symbols as in Fig. 6.)

In conclusion, we have experimentally investigated the power injected in a bistable colloidal system by an external oscillating force. We find that the injected power in the stochastic resonance regime presents a maximum when the frequency of the driving force corresponds to half of the Kramers' rate. We have compared the stochastic work and the classical work for different frequencies and shown that although the average values of each work are equal, the distributions of work reveal some differences. They present large tail toward negative values and their shape are non-gaussian close to the resonance when averaging over a single period. Analyzing in more details the distribution of work and dissipated heat, we have tested the validity of SSFT for a non-linear potential. We have shown that FT rapidly converge to the asymptotic value for rather small n. The fact that for the total entropy W_{sn}/T, SSFT is not satisfied exactly for small n is certainly due to statistical and numerical inaccuracy. We have also shown that the SSFT is only valid for small values of dissipated heat compared to the mean value at long time. It would be interesting to change the symmetry of the driving force cycle [26] to explore the limit of the FT.

We acknowledge useful discussion with R. Benzi, K. Gawedzki and S. Joubaud. This work has been partially supported by ANR-05-BLAN-0105-01.

REFERENCES

[1] A. Simon, A. Libchaber, Phys. Rev. Lett., 68, 3375 (1992).
[2] R.Benzi,G. Parisi, A. Sutera,A. Vulpiani, SIAM J. Appl. Math., 43, 565 (1983).
[3] L. Gammaitoni, F. Marchesoni and S. Santucci. Phys. Rev. Lett. **74** (7), 1052-1055 (1995).
[4] D. Babic, C. Schmitt, I. Poberaj and C. Bechinger. Europhys. Lett. **67** (2), p. 158 (2004).
[5] T. Iwai. Physica A **300**, pp. 350-358 (2001)
[6] D. Dan and A. M. Jayannavar. Physica A **345**, pp. 404-410 (2005)
[7] D. J. Evans, E. G. D. Cohen, and G. P. Morriss, *Phys. Rev. Lett.* **71**, 2401 (1993); D. J. Evans and D. J. Searles, *Phys. Rev. E* **50**, 1645 (1994).
[8] G. Gallavotti, E. G. D. Cohen. Phys. Rev. Lett. **74**, pp. 2694 - 2697 (1995).
[9] Jorge Kurchan. J. Phys. A: Math. Gen. **31**, 3719 (1998). J. L. Lebowitz and H. Spohn, *J. Stat. Phys.* **95**, 333 (1999).
[10] F. Ritort J. Phys.: Condens. Matter **18**, R531 (2006).
[11] R. van Zon and E.G.D. Cohen, *Phys. Rev. Lett.* **91** (11) 110601 (2003); R. van Zon, S. Ciliberto, E.G.D. Cohen, *Phys. Rev. Lett.* **92** (13) 130601 (2004).
[12] G.M. Wang, E.M. Sevick, E. Mittag, D. J. Searles and D. J. Evans. Phys. Rev. Lett. **89**, 050601 (2002)
[13] V. Blickle, T. Speck, L. Helden, U. Seifert and C. Bechinger. Phys. Rev. Lett. **96**, 070603 (2006).
[14] A. Imparato, L. Peliti, G. Pesce, G. Rusciano, A. Sasso, cond-mat/0707.0439v2.
[15] F. Douarche, S. Joubaud, N. B. Garnier, A. Petrosyan, and S. Ciliberto Phys. Rev. Lett. **97** (14), 140603 (2006).
[16] N. Garnier, S. Ciliberto, *Phys. Rev. E* **71** 060101(R) (2005).
[17] S. Schuler, T. Speck, C. Tietz, J. Wrachtrup and U. Seifert. Phys. Rev. Lett. **94**, 180602 (2005).
[18] T. Speck, V. Blickle, C. Bechinger and U. Seifert, Europhys.Lett, **79**, 30002 (2007).
[19] S. Saikia, R. Roy and A. M. Jayannavar. Arxiv : cond-mat/0701303v1 (2007).
[20] M. Sahoo, S. Saikia, M. C. Mahato and A. M. Jayannavar Arxiv : cond-mat/0708.0496v1 (2007).
[21] K. Sekimoto J. Phys. Soc. Jpn. **66** (5), 1234 (1997).
[22] S. Taniguchi, E.G.D.Cohen,Arxiv:0708.2940V2
[23] U. Seifert Phys. Rev. Lett., **95** 040602 (2005).
[24] C. Schmitt, B. Dybiec, P. Hänggi and C. Bechinger. Europhys. Lett. **74** (6), p. 937 (2006).
[25] S. Joubaud, N. B. Garnier and S. Ciliberto Arxiv:0711.2388.
[26] T. Mai and A. Dhar. Phys. Rev. E **75**, 061101 (2007)